†On leave at the Department of Applied Physics, Hansen Laboratories, Stanford University, Stanford, Calif. 94305. The hospitality of Professor S. Doniach and the support of the John Simon Guggenheim Memorial Foundation are gratefully acknowledged.

‡Presently at Sandia Laboratories, Albuquerque, N. M. 87115.

[1]M. E. Fisher, J. Math. Phys. 5, 944 (1964).

[2]M. E. Fisher, Rep. Progr. Phys. 30, 615 (1967).

[3]L. P. Kadanoff *et al.*, Rev. Mod. Phys. 39, 395 (1967).

[4]W. J. Camp and M. E. Fisher, Phys. Rev. Lett. 26, 73 (1971). This article will be referred to as I and we will employ the same notation here.

[5]T. T. Wu, Phys. Rev. 149, 380 (1966); L. P. Kadanoff, Nuovo Cimento 44, B276 (1966); H. Cheng and T. T. Wu, Phys. Rev. 164, 719 (1967); J. Stephenson, J. Math. Phys. 7, 1123 (1966); R. Hecht, Phys. Rev. 158, 557 (1967); R. Hartwig and M. E. Fisher, Advan. Chem. Phys. 15, 333 (1969), and Arch. Ration. Mech. Anal. 32, 190 (1969).

[6]We have considered explicitly the two-dimensional square Ising model with ferromagnetic second-neighbor interactions in the layers perpendicular to the direction $\vec{R}$.

[7]We consider d-dimensional hypercubic lattices with surfaces perpendicular to the cubic axes. When $d=3$ the case $(d_\perp=1, d_\parallel=2)$ describes correlations near a single planar surface; $(d_\perp=2, d_\parallel=1)$ means that both $\vec{R}_1$ and $\vec{R}_2$ lie near the intersection of two plane surfaces, that is, near a one-dimensional edge of the simple cubic lattice. Note that $d_\perp=0$ always implies the bulk situation.

[8]To our knowledge these phenomenological predictions have not previously been reported.

[9]For further references see I.

[10]A preliminary report of this approach and its initial results was made by M. E. Fisher, J. Phys. Soc. Jap., Suppl. 26, 87 (1969).

[11]As in I we assume $\vec{R}$ lies in a direction close to the axis along which the lattice is built up. The perturbation theory generates successive angular corrections.

[12]We may also recall that the interfacial tension vanishes as $T \to T_c$, thus enhancing such fluctuations (see also Ref. 10).

Diffraction Systematics of Nuclear and Particle Scattering

W. E. Frahn
Physics Department, University of Cape Town, Rondebosch, C. P., South Africa
(Received 14 December 1970)

It is shown that, contrary to popular belief, diffraction scattering in nuclear and particle physics is not always of Fraunhofer type. By establishing a simple physical connection between scattering in a Coulomb field and Fresnel diffraction we show that diffractive collisions of heavy charged particles are predominantly of Fresnel type. We derive quantitative criteria for Fraunhofer and Fresnel scattering which lead to a new classification of all scattering processes.

Diffraction effects in nuclear and particle scattering have been known for a long time and are believed to be well understood. At high enough energy, elastic scattering can be regarded as shadow scattering in the presence of a large number of nonelastic processes; thus diffraction is a consequence of the unitarity of the scattering matrix. It is commonly assumed that all diffraction scattering is of Fraunhofer type. The argument is simple[1]: In all nuclear scattering situations the particle source and the point of observation are practically at "infinity" relative to the dimensions of the scattering object. If the energy is high enough such that the wavelength is small compared to the radius of the interaction region, it seems obvious that we have the conditions for Fraunhofer diffraction.

However, several years ago it was noticed[2] that well-known features in the angular distributions for scattering of complex nuclei closely resemble the characteristics of Fresnel diffraction in optics. It was shown that these "Fresnel effects" are associated with the Coulomb interaction. In a certain well-defined limit, which corresponds to high energy and a strong Coulomb field, the analytic expression in the strong-absorption model[3] for the ratio of the differential scattering cross section $\sigma(\theta)$ to the Rutherford cross section $\sigma_R(\theta)$ reduces to the simple formula

$$\sigma(\theta)/\sigma_R(\theta) = \tfrac{1}{2}\{[\tfrac{1}{2}-C(w)]^2+[\tfrac{1}{2}-S(w)]^2\}, \quad (1)$$

where $C(w)$ and $S(w)$ are the Fresnel integrals of argument

$$w = (\Lambda/\pi \sin\theta_c)^{1/2} (\theta - \theta_c). \tag{2}$$

Equation (1) is the limiting expression for the simplest case of a completely absorbing, sharp-edged nucleus with cutoff angular momentum Λ and critical angle θ_c. Although in actual scattering situations the ideal pattern (1) is somewhat modified by the diffuseness of the nuclear surface and by real nuclear phase shifts, there is clear experimental evidence[2,4-7] for the presence of "Fresnel effects" in the angular distributions for elastic scattering of heavy ions (see, for example, Baker and McIntyre[8] and Fig. 1).

Equation (1) has the same form as the intensity distribution of light diffracted by the edge of an opaque screen or convex body in the vicinity of the shadow cone. Is there a physical reason behind this analogy? Because of the earlier argument for Fraunhofer conditions this appears to be merely a formal coincidence. However, it is quite easy to see that *there is a direct physical relation between scattering in a Coulomb field and Fresnel diffraction.* The Coulomb field distorts the incoming wave in such a way that the effective wave front over the interaction region is no longer plane but appreciably curved. Under these conditions, diffraction scattering changes from Fraunhofer to Fresnel type. In a semiclassical picture, particles scattered

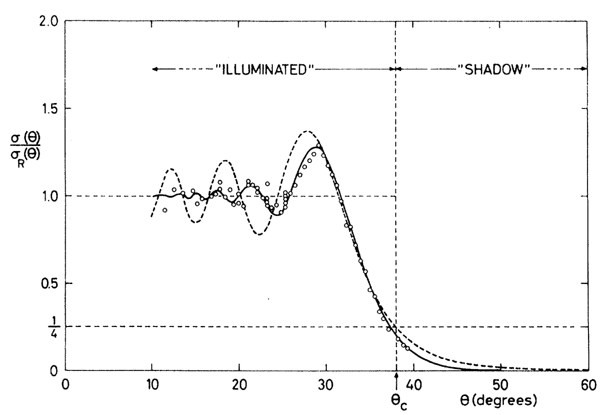

FIG. 1. Fresnel diffraction pattern in heavy-ion scattering. The experimental data for $^{16}O + ^{208}Pb$ elastic scattering at $E_L = 170.1$ MeV are taken from Ref. 8. The solid curve is a strong-absorption model fit (Ref. 3), the broken curve is calculated from Eqs. (1) and (2), both with $n = 31.2$ and $\Lambda = 90.4$. The figure illustrates to what extent the characteristic features of the idealized Fresnel limit (1) are preserved at finite energy despite modification by the effects of surface diffuseness ($\Delta = 3.41$) and real nuclear phase shifts ($\mu/4\Delta = 0.33$).

through the grazing angle θ_c *appear to originate from a virtual point source situated at a finite distance from the scattering center.* Simple considerations on the geometry of Coulomb scattering show that this distance is $d = b_c/\sin\theta_c$, where b_c is the impact parameter of the grazing trajectory. Thus the Coulomb field near the nuclear surface acts like a diverging lens of focal length $b_c \cot\theta_c$. Furthermore, it turns out that the impact parameter b_c [*not*, as one might expect, the interaction radius R (!)] is the effective radius of the nuclear diffraction problem. It then follows immediately from the familiar formulas for Fresnel diffraction in physical optics that the scattering intensity in the vicinity of θ_c is given by Eq. (1) with precisely the argument (2).

The condition for Fraunhofer and Fresnel diffraction can be stated as follows.[1] Let a be the radius of the interaction region and d the shorter of the two distances d_1, from the source point to the scattering center, and d_2, from the observation point to the scattering center. A general requirement for diffraction is the short-wavelength condition $ka \gg 1$. The type of diffraction pattern is then determined by the parameter $p = ka^2/d$, and we have Fraunhofer diffraction if $p \ll 1$, Fresnel diffraction if $p \gtrsim 1$. In the case of nuclear and particle scattering, with $a = b_c$ and $d = b_c/\sin\theta_c$, these conditions become

$$\Lambda \gg 1, \quad \Lambda \sin\theta_c \ll 1, \text{ Fraunhofer scattering,}$$
$$\Lambda \gg 1, \quad \Lambda \sin\theta_c \gtrsim 1, \text{ Fresnel scattering,} \tag{3}$$

where $\Lambda = kb_c$ is the "cutoff" angular momentum familiar from strong-absorption models.[3,9] Since the critical angle θ_c is given by $\theta_c = 2\tan^{-1}(n/\Lambda)$, where $n = Z_1Z_2\alpha/\beta$ is the Coulomb parameter [$\alpha = 1/137$, $\beta = $ (relative velocity)$/c$], conditions (3) mean, roughly, that Fraunhofer-type scattering occurs for weak Coulomb fields, Fresnel-type scattering for strong Coulomb fields. Thus it is the Coulomb interaction which essentially determines the "optics" of the scattering process.

However, we see that in general *two* parameters, Λ and $p = \Lambda \sin\theta_c$, are needed to specify a scattering situation with regard to its diffraction characteristics. This enables us to classify all scattering situations of charged particles above the Coulomb barrier by means of a "diffraction diagram." It is convenient to choose as parameters, because of their direct physical meaning, the Coulomb parameter n and the ratio $h = E/V_c$, where E is the c.m. kinetic energy and $V_c = Z_1 Z_2 e^2/R$ is the Coulomb barrier potential. The quantities Λ and p are related to these parameters by

$$\Lambda = 2nh(1-h^{-1})^{1/2}, \quad p = 2n[1-(2h-1)^{-2}]. \tag{4}$$

In the n-h diagram the curves $\Lambda=$ const and $p=$ const form a net of parameter lines which define regions of different diffractive character. We distinguish three main regions: (I) $\Lambda \lesssim 10$, nondiffractive scattering; (II) $\Lambda \gtrsim 10$ and $p \lesssim 0.1$, Fraunhofer scattering; and (III) $\Lambda \gtrsim 10$ and $p \gtrsim 1$, Fresnel scattering. The angular distributions for scattering situations corresponding to these regions are characteristically different: A differential cross section $\sigma(\theta)$ in region I has few oscillations and no pronounced forward-backward asymmetry, while one in region II is strongly forward peaked and, at least for complex nuclei as tragets, has large regular oscillations of period π/Λ, which are damped to some extent by contributions from the real part of the scattering amplitude. In region III, the angular distributions are characterized by three main features[2]: (i) a pronounced "rise" of $\sigma(\theta)$ above the Rutherford cross section at an angle $\theta_r \simeq \theta_c - (3\pi \sin\theta_c/2\Lambda)^{1/2}$, (ii) the "one-quarter point" property[9] $\sigma/\sigma_R \simeq \frac{1}{4}$ at $\theta = \theta_c$, and (iii) a strong (almost exponential) monotonic decrease in the "shadow region" $\theta > \theta_c$. It should be noted, however, that the three main regions have no sharply defined boundaries; they are connected by transition zones in which the diffractive character changes gradually from one type to another.

All of these features are well known from the vast experimental literature on elastic scattering. However, our diffraction conditions (3) now provide *quantitative criteria* for their occurrence. For any given scattering situation, the representative point in the diffraction diagram determines the overall shape of the angular distribution.[10] Thus it becomes possible to make *specific predictions* about the form of $\sigma(\theta)$ obtainable with future accelerator facilities. Note that the classification by means of the diffraction diagram is model independent, as it depends only on general wave-mechanical properties of scattering and on the interaction radius R. The latter is the strong absorption radius defined by $\mathrm{Re}\,\eta(\Lambda) = \frac{1}{2}$ which was recently shown to be the significant size parameter for scattering.[11]

Figure 2 shows the diffraction diagram with the main regions I, II, and III, together with several areas corresponding to scattering situations of physical interest: (i) scattering of nuclei by

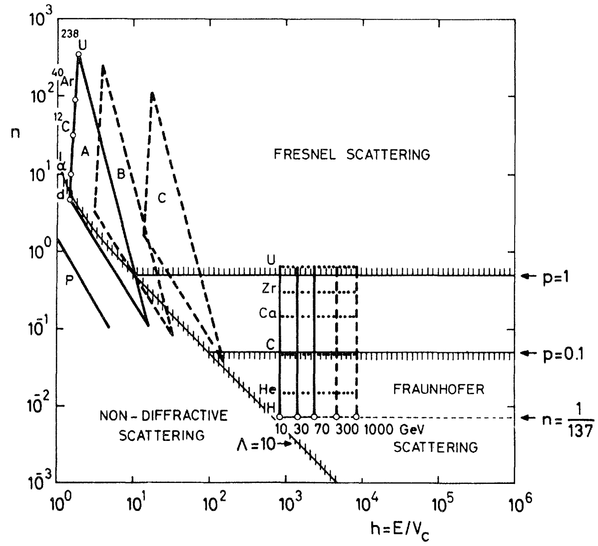

FIG. 2. Diffraction diagram for scattering of charged particles above the Coulomb barrier. The ordinate is the Coulomb parameter n, the abscissa is the ratio of the c.m. kinetic energy E to the Coulomb barrier energy V_c. The picket-fence lines delimit the regions corresponding to nondiffractive scattering and diffractive scattering of Fresnel and Fraunhofer type. Because of the gradual changes in diffractive behavior these lines should not be regarded as sharply defined boundaries. The triangular areas A, B, and C represent the scattering of composite particles (deuterons to ^{238}U ions) by nuclei at $E_L = 10$, 20, and 100 MeV/nucleon, respectively; the line labelled P corresponds to proton-nucleus scattering at 10 MeV. The vertical lines represent the scattering of protons (and other singly charged hadrons) by protons and complex nuclei at E_L between 10 and 1000 GeV. The dotted horizontal line at $n = \alpha = 1/137$ is the trajectory for hadron-hadron scattering in the asymptotic energy region.

nuclei at laboratory energies E_L of 10 MeV/nucleon (A), 20 MeV/nucleon (B), and 100 MeV/nucleon (C), (ii) scattering of protons by nuclei at 10 MeV, and (iii) the relativistic region for scattering of singly charged hadrons by protons and complex nuclei with laboratory kinetic energies in the range 10-1000 GeV. The latter region has as its lower boundary the minimum value of the Coulomb parameter $n = \alpha = 1/137$.

It is clear from Fig. 2 that proton-nucleus scattering is nondiffractive at lower energies but becomes diffractive above about 50 MeV for heavy target nuclei. The scattering of singly charged hadrons in the multi-GeV region is fully diffractive. It is predominantly of Fraunhofer type and remains so all the way up into the asymptotic region.

Because of the topical interest in experiments with present and future heavy-ion facilities we

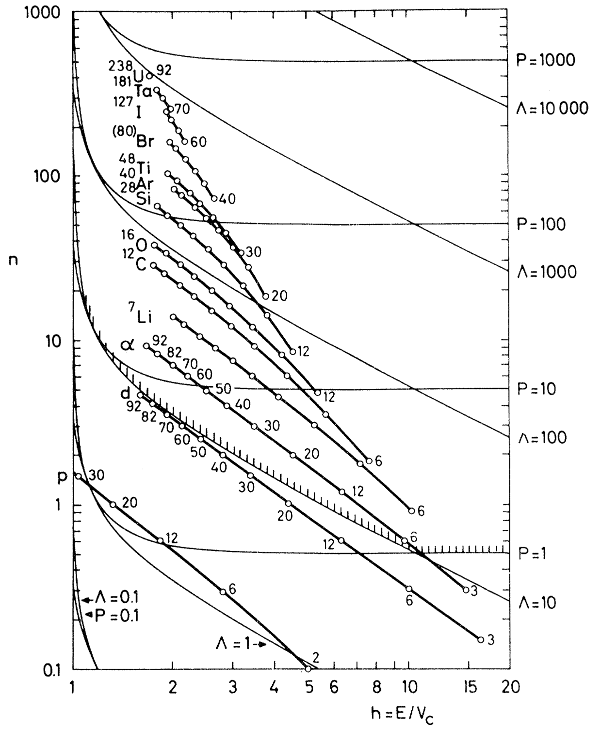

FIG. 3. Diffraction diagram for nucleus-nucleus scattering at $E_L = 10$ MeV/nucleon. Parameter curves are shown for constant values of the diffraction parameters Λ and p defined in the text. The picket-fence line indicates the approximate lower boundary of the Fresnel-scattering region. Solid lines represent the scattering of a given projectile (identified by its symbol ^{A}X at the upper left end) by a range of target nuclei (labelled by their atomic numbers Z_2). For instance, the scattering situation of Fig. 1 is represented by the point second from left on the ^{16}O curve.

show in Fig. 3 a section of the diffraction diagram with representative points corresponding to scattering of various projectiles (deuterons to ^{238}U ions) at $E_L = 10$ MeV/nucleon by a range of target nuclei. It is seen that all collisions between heavy ions lie well inside the Fresnel region, and we conclude that *the diffractive scattering of heavy nuclei is predominantly of Fresnel type.* The uppermost point in Fig. 3 represents the collision between two ^{238}U nuclei and has index of Fresnel character $p = 714$ compared with $p = 55.7$ for $^{16}O + {}^{208}Pb$ scattering (Fig. 1). We therefore expect that the angular distributions for scattering of uranium ions and of other heavy nuclei with high index of Fresnel character p will closely approximate the limiting pattern described by Eq. (1).

---

[1]See, for example, L. Van Hove, in *High Energy Physics and Nuclear Structure,* edited by G. Alexander (North-Holland, Amsterdam, 1967), p. 259.

[2]W. E. Frahn, Nucl. Phys. 75, 577 (1966).

[3]W. E. Frahn and R. H. Venter, Ann. Phys. (New York) 24, 243 (1963); W. E. Frahn, in *Fundamentals in Nuclear Theory,* edited by A. de-Shalit and C. Villi (International Atomic Energy Agency, Vienna, Austria, 1967), p. 3.

[4]D. A. Bromley, in *Nuclear Structure and Nuclear Reactions,* edited by M. Jean and R. A. Ricci (Academic, New York, 1969), p. 242.

[5]J. O. Newton, Progr. Nucl. Phys. 11, 53 (1970).

[6]M. H. Simbel and A. Y. Abul-Magd, Nucl. Phys. A120, 152 (1968).

[7]E. V. Inopin and A. V. Shebeko, Yad. Fiz. 11, 140 (1970), [Sov. J. Nucl. Phys. 11, 78 (1970)].

[8]S. D. Baker and J. A. McIntyre, Phys. Rev. 161, 1200 (1967); S. D. Baker, thesis, Yale University, 1963 (unpublished).

[9]J. S. Blair, Phys. Rev. 95, 1218 (1954).

[10]Except for structure effects and resonances with affect angular distributions in regions II and III mainly at backward angles.

[11]J. S. Blair, in *Nuclear Reactions Induced by Heavy Ions,* edited by R. Bock and W. R. Hering (North-Holland, Amsterdam, 1970), p. 1; D. F. Jackson, *Nuclear Reactions* (Methuen and Co., London, 1970), Chap. 8, and references cited therein.